Hindawi
Shock and Vibration
Volume 2019, Article ID 7082538, 8 pages
https://doi.org/10.1155/2019/7082538

Research Article

Frequency-Domain-Based Nonlinear Response Analysis of Stationary Ring Displacement of Noncontact Mechanical Seal

Dian Feng Sun, Jian Jun Sun, Chen Bo Ma, and Qiu Ping Yu

School of Mechanical and Electronic Engineering, Nanjing Forestry University, Nanjing, Jiangsu 210037, China

Correspondence should be addressed to Jian Jun Sun; sunjianjun@njfu.edu.cn

Received 13 July 2019; Accepted 26 September 2019; Published 18 November 2019

Guest Editor: Franco Concli

Dynamic characteristics affect the operational reliability of noncontacting mechanical seals, which involves the complex relationship between the system of noncontact mechanical seals, excitation, and response. Hence, it is one of the hot topics of current research. However, domestic and foreign scholars mainly calculate the response in the time domain by establishing a linear dynamic model so that the response results can be used for system stability and tracking analysis. In this study, according to the harmonic excitation, the stationary ring's output response was expressed via the famous Volterra series and solved with a new method, which can be used to analyze the frequency response and to calculate the displacement response of the stationary ring with single and double harmonic excitation. Based on the analysis of the response results, the parameter (stationary ring mass, axial damping, stiffness, etc.) selection scheme of noncontact mechanical seals at high and low frequencies was obtained.

1. Introduction

During operation, the moving and stationary rings, which constitute the noncontact mechanical seals in rotating machines such as centrifugal compressors, pumps, aircraft engines, and nuclear main pumps, are not in contact; the friction and wear are small; the service life is long; and the leakage rate is controllable [1, 2]. It has been widely used and has become the focus of scholars at home and abroad. The long-life, safe, and reliable operation of the noncontact mechanical seal relies on the fluid dynamic pressure formed between the stationary and dynamic rings on the one hand and the good dynamic performance on the other hand. Through continuous research, people have laid a rich theoretical foundation and accumulated engineering experience in fluid dynamic pressure film formation on the surface of stationary and dynamic rings, which provides the noncontact mechanical seal with good working life and low leakage rate under stable conditions.

At present, domestic and foreign scholars mainly rely on the noncontact mechanical seal-operating conditions (pressure, rotational speed, etc.), the stationary axial force caused by the research object (microscopic cavitation, end-face contact, etc.) is the excitation, and the response in the time domain is solved accordingly. It is used to analyze the stability and follow-up of the system, and finally to determine the leakage of the system, or to provide a basis for material selection and structural design of the stationary ring. Menget al. [3], Xuexing et al. [4], and Falaleev and Vinogradov [5], respectively, obtained the axial force in the stationary ring time domain with the axial force generated via the sealing fluid-solid effect, microcavitation, end-face contact, and external sinusoidal excitation. The response is used to analyze system stability and determine system leakage. Varney and Green [6], Songtao et al. [7], and Badykov and Falaleev [8], respectively, used the pressure caused by the change of the rotating shaft speed, the stationary unbalanced force of the stationary ring caused by the pressure difference between the inside and outside of the sealed cavity, and the speed step as the excitation, and calculated the stationary ring time. The response within the domain is used to analyze the follow-up of the dynamic and stationary ring and to acquire system leakage. Feng and Yizheng [9], Green and Barnsby [10, 11], and Blasiak [12] calculated the stationary ring structure and selected the stationary ring material by applying axial excitation and also

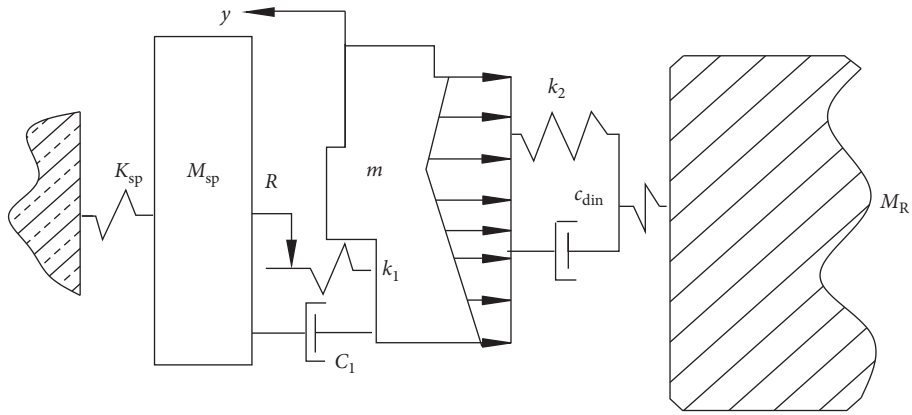

Figure 1: Model of stationary ring displacement response in frequency domain analysis of noncontact mechanical seal.

calculated the stationary ring displacement response which determines the leakage rate of the system in the time domain according to the allowable value of the response. In fact, the material selection and structural design of the stationary ring also need to consider the effects of various excitations in the high- and low-frequency bands. In summary, although a large number of stationary-displacement response studies based on the time domain are carried out to analyze the stability of the system, relevant theories and experiences supporting the design and operation of common noncontact mechanical seals have been obtained. However, because of the complexity of the system, the multifrequency of the excitation, and the uncertainty of the response, the previous results are difficult to adapt to complex and harsh working environments, such as high-speed aircraft engines, nuclear main pumps with seismic load risk (disengagement), or impact. It can be seen that the response of the stationary ring displacement of the noncontact mechanical seal in the frequency domain is of great significance for analyzing the leakage rate of the system.

In this article, the relationship between excitation and response in the stationary ring time domain is given by the Volterra series multiconvolution integral, and the multidimensional Fourier transform is implemented for the multiple convolution integral. An expression for the response of the stationary ring in the frequency domain is obtained. To solve this equation, the Volterra frequency domain kernel is derived. According to the single-set and dual-frequency harmonic excitation, by calculating the response linearly and nonlinearly and discussing the noise situation, the results are analyzed. The parameter selection (stationary ring mass, axial damping, stiffness, etc.) scheme of the noncontact mechanical seal under high- and low-frequency operation is obtained.

2. Physical Model

The structural model for analyzing the stationary ring displacement response in the frequency domain is shown in Figure 1 and the symbols are shown in Table 1. The gas film between the rotating M_R and the stationary rings m, the O-rings between the stationary rings m and the M_{PS} followers (including sleeves and springs), are considered to have certain stiffness and damping.

3. Theoretical Basis

3.1. Governing Equation. During the operation of the noncontact mechanical seal, internal excitation such as cavitation or condensation of the fluid film, pressure fluctuation of the sealing medium, or the blocking fluid, and external excitation such as seismic load and external impact load may cause the movement of stationary ring. The relationship between the output response $y(t)$ and the input stimulus $x(t)$ is the Volterra series multiple convolution integral:

$$y(t) = \sum_{n=1}^{\infty} \int_{-\infty}^{+\infty} \cdots \int_{-\infty}^{+\infty} h_n(\tau_1, \cdots, \tau_n) \prod_{i=1}^{n} x(t-\tau_i) \mathrm{d}\tau_1 \cdots \tau_n, \tag{1}$$

where $h_n(\tau_1, \ldots, \tau_n)$ is called the nth-order Volterra time-varying kernel function.

From the Volterra series theory, the time-varying kernel function $h_n(\tau_1, \tau_2, \ldots, \tau_n)$ implements a multidimensional Fourier transform to

$$H_n(j\omega_1, \ldots, j\omega_n) = \int_{-\infty}^{+\infty} \cdots \int_{-\infty}^{+\infty} h_n(\tau_1, \cdots, \tau_n) \cdot \left(\exp\left(-j\omega_1\tau_1 + \cdots + j\omega_n\tau_n\right)\right) \mathrm{d}\tau_1 \cdots \tau_n. \tag{2}$$

Among them, $H_n(w_1, \ldots, w_n)$ is called the nth-order generalized frequency-domain response function, also known as the nth-order Volterra frequency domain kernel. The Fourier transform of the output response $y(t)$ is given as follows:

$$\begin{aligned} Y(j\omega) = {} & R_1\left[H_1(j\omega_1)X(j\omega_1)\right] \\ & + R_2\left[H_2(j\omega_1, j\omega_2)X(j\omega_1)X(j\omega_2)\right] \\ & + \cdots + R_n\left[H_n(j\omega_1, \cdots, j\omega_n)\prod_{i=1}^{n} X(j\omega_i)\right] + \cdots. \end{aligned} \tag{3}$$

Define R_n as the nth order output spectrum.

The excitation selected in this study is given as follows:

$$x(t) = e^{jwt}. \tag{4}$$

Substituting equation (4) into equation (3), the response of the system is given as follows:

$$\begin{aligned} Y(j\omega) = {} & H_1(j\omega)e^{jwt} + H_2(j\omega, j\omega)e^{j2wt} + \cdots \\ & + H_3(j\omega, j\omega, j\omega)e^{j3wt} + \cdots, \end{aligned} \tag{5}$$

where equation (5) is nonlinear analysis, whereas (6) is linear analysis, which is given as follows:

$$Y(j\omega) = H_1(j\omega)e^{jwt}. \tag{6}$$

3.2. Stationary Ring Response under Noise Excitation. The input stimulus is given as follows:

$$x(t) = e^{jw_1t} + e^{jw_2t}. \tag{7}$$

Substituting (7) into (3), the response of the system is given as follows:

$$\begin{aligned} Y(j\omega) = {} & H_1(j\omega_1)e^{jw_1t} + H_1(j\omega_2)e^{jw_2t} \\ & + H_2(j\omega_1, j\omega_1)e^{j2w_1t} + H_2(j\omega_1, j\omega_2)e^{j(w_1+w_2)t} \\ & + H_2(j\omega_2, j\omega_2)e^{j2w_2t} + H_3(j\omega_1, j\omega_1, j\omega_1)e^{j3w_1t} \\ & + 3H_3(j\omega_1, j\omega_1, j\omega_2)e^{j(2w_1+w_2)t} \\ & + 3H_3(j\omega_1, j\omega_2, j\omega_2)e^{j(w_1+2w_2)t} \\ & + H_3(j\omega_2, j\omega_2, j\omega_2)e^{j3w_2t} \cdots. \end{aligned} \tag{8}$$

It is known from equations (5) and (8) that to calculate the output response spectrum $Y(jw)$, it is necessary to first calculate the Volterra frequency domain kernels of each order. In order to facilitate the calculation, it is assumed that the noncontact mechanical seal operates stably. Before the excitation disturbance is introduced, the axial displacement and initial velocity of the stationary rings are zero, and the mass of the stationary rings is 1 kg. Assuming that the stiffness has strong nonlinearity due to the rotating ring and the stationary ring, the dynamic equation is given as follows:

$$\begin{cases} m\dfrac{\mathrm{d}^2y(t)}{\mathrm{d}t^2} + C\dfrac{\mathrm{d}y(t)}{\mathrm{d}t} + Ky(t) + by^3(t) = x(t), \\ y(t) = 0, \\ \dfrac{\mathrm{d}y(t)}{\mathrm{d}t}|t = 0, m = 1, \end{cases} \tag{9}$$

where m is the static ring mass, C is the total axial damping, K is the total axial stiffness, and b is the nonlinear stiffness. Assuming that (1) is the solution of (9), the derivative formula containing the parameter integral is repeatedly used in (1) to obtain $\mathrm{d}y(t)/\mathrm{d}t$, $\mathrm{d}^2y(t)/\mathrm{d}t$, and $y^3(t)$ is derived from the binomial theorem. Then, substitute $\mathrm{d}y(t)/\mathrm{d}t$, $\mathrm{d}^2y(t)/\mathrm{d}t$, and $y^3(t)$ into (9), compare the coefficients on both sides of the equation, and obtain a set of linear coefficients that determine the kernel $h_n(\tau_1, \ldots, \tau_n)$ of each order. The differential equation is given as follows:

$$h_1^{''}(\tau) + Ch_1'(\tau) + Kh_1(\tau) = 0, \tag{10}$$

$$\begin{aligned} & \left(\frac{\partial^2}{\partial\tau_1^2} + \frac{\partial^2}{\partial\tau_1\partial\tau_2} + \frac{\partial^2}{\partial\tau_2^2}\right)h_2(\tau_1, \tau_2) + C\left(\frac{\partial}{\partial\tau_1} + \frac{\partial}{\partial\tau_2}\right)h_2(\tau_1, \tau_2) \\ & + Kh_2(\tau_1, \tau_2) = 0, \end{aligned} \tag{11}$$

$$\begin{aligned} & \left(\frac{\partial^2}{\partial\tau_1^2} + \frac{\partial^2}{\partial\tau_2^2} + \frac{\partial^2}{\partial\tau_2^3} + \frac{\partial^2}{\partial\tau_1\partial\tau_2} + 2\frac{\partial^2}{\partial\tau_2\partial\tau_3} + \frac{\partial^2}{\partial\tau_1\partial\tau_3}\right)h_3(\tau_1, \tau_2, \tau_3) \\ & + C\left(\frac{\partial}{\partial\tau_1} + \frac{\partial}{\partial\tau_2} + \frac{\partial}{\partial\tau_3}\right)h_3(\tau_1, \tau_2, \tau_3) + Kh_3(\tau_1, \tau_2, \tau_3) \\ & + b\prod_{i=1}^{3}h_i(\tau_i) = 0, \end{aligned} \tag{12}$$

$$\begin{aligned} & \left(\frac{\partial^2}{\partial\tau_1^2} + \frac{\partial^2}{\partial\tau_2^2} + \frac{\partial^2}{\partial\tau_2^3} + \frac{\partial^2}{\partial\tau_2^4} + \frac{\partial^2}{\partial\tau_2^5} + 2\frac{\partial^2}{\partial\tau_1\partial\tau_2} + 2\frac{\partial^2}{\partial\tau_1\partial\tau_3}\right. \\ & + 2\frac{\partial^2}{\partial\tau_1\partial\tau_4} + 2\frac{\partial^2}{\partial\tau_1\partial\tau_5} + 2\frac{\partial^2}{\partial\tau_2\partial\tau_3} + 2\frac{\partial^2}{\partial\tau_2\partial\tau_4} + 2\frac{\partial^2}{\partial\tau_2\partial\tau_5} \\ & \left. + 2\frac{\partial^2}{\partial\tau_3\partial\tau_4} + 2\frac{\partial^2}{\partial\tau_3\partial\tau_5} + 2\frac{\partial^2}{\partial\tau_4\partial\tau_5}\right)h_5(\tau_1, \ldots, \tau_5) \\ & + C\left(\frac{\partial}{\partial\tau_1} + \frac{\partial}{\partial\tau_2} + \frac{\partial}{\partial\tau_3} + \frac{\partial}{\partial\tau_4} + \frac{\partial}{\partial\tau_5}\right)h_5(\tau_1, \ldots, \tau_5) \\ & + Kh_5(\tau_1, \ldots, \tau_5) + 3bh_3(\tau_1, \tau_2, \tau_3)h_4(\tau_4)h_5(\tau_5) \\ & + 3bh_1(\tau_1)h_2(\tau_2, \tau_3)h_2(\tau_4, \tau_5) = 0. \end{aligned} \tag{13}$$

Perform Fourier transform on (10), (11), (12), and (13) and consider the initial conditions to obtain the first five-order Volterra frequency domain kernel as given as follows:

$$H_1(j\omega) = \frac{1}{-\omega^2 + Cj\omega + K}. \tag{14}$$

As (7) is a homogeneous equation,

$$H_2(j\omega_1, j\omega_2) = 0,$$

$$H_{2n}(j\omega_1, j\omega_2, \ldots, j\omega_{2n}) = 0,$$

$$H_3(j\omega_1, j\omega_2, j\omega_3) = \frac{-b}{(j\omega_1 + j\omega_2 + j\omega_3)^2 + C(j\omega_1 + j\omega_2 + j\omega_3) + K} H_1(j\omega_1)H_2(j\omega_2)H_3(j\omega_3), \tag{15}$$

$$H_5(j\omega_1, \cdots, j\omega_5) = \frac{-3b}{(j\omega_1 + j\omega_2 + j\omega_3)^2 + C(j\omega_1 + j\omega_2 + j\omega_3) + K} H_3(j\omega_1, j\omega_2, j\omega_3)H_4(j\omega_4)H_5(j\omega_5).$$

4. Numerical Calculation and Analysis of Results

Select stationary ring mass $m = 0.125\,\text{kg}\sim0.2\,\text{kg}$, total axial damping $C = 30\,\text{N·s/m}\sim150\,\text{N·s/m}$, total axial linear stiffness $15000\,\text{N/m}\sim20000\,\text{N/m}$, excitation amplitude $\text{Ar} = 30\,\mu\text{m}–100\,\mu\text{m}$, excitation frequency $w_1 = 1\,\text{rad/sec}$, $w_2 = 2\,\text{rad/sec}$, and nonlinear stiffness $b = 10^{15}\,\text{N/m}^3$.

4.1. Linear Analysis for Stationary Ring Response. When the noncontact mechanical seal is operated, it is necessary to select reasonable system characteristic parameters (stationary ring mass, axial damping, linear stiffness, etc.) according to the frequency of the mechanical seal operation. Figures 2(a)–2(d) show the effect of different excitation amplitudes, stationary ring mass, axial damping, and linear stiffness on the output response of the stationary ring axial displacement in the frequency domain during linear analysis and show that the frequency is close to the natural frequency of the system. The stationary ring reaches the output-displacement response peak. As can be seen from Figure 2(a), the system parameters (stationary ring mass, axial damping, and linear stiffness) are fixed; the larger the excitation amplitude corresponding to the same frequency, the larger will be the stationary ring output-displacement response. Figure 2(b) shows that the parameters (excitation amplitude, axial damping, and linear stiffness) are fixed, and as the mass of the stationary ring increases, the frequency of the stationary ring output displacement response peak value $Y(jw)$ decreases. This is because for the same vibration energy, the mass of the stationary rings will be smaller speed and, therefore, may produce a larger displacement in the lower frequency range. Figure 2(c) shows that the parameters (excitation amplitude, stationary ring mass, and linear stiffness) are fixed, and the larger the total axial damping, the wider will be the bandwidth of the resonance region. This shows that the damping ratio is small, the quality factor is high, the resonance region is narrow, and the resonance peak is steep; the damping ratio is large, the quality factor is low, the resonance region is wide, and the resonance is flat. Figure 2(d) shows that the parameters (excitation amplitude, stationary ring mass, and axial damping) are fixed, and the greater the linear stiffness, the greater is the natural frequency. The frequency ratio is a decreasing function in the pre-resonance region and an increasing function in the postresonance region; so reducing the stationary ring displacement cannot increase the linear stiffness in discriminately.

4.2. Nonlinear Analysis for Stationary Ring Response. Figures 3(a)–3(d) show the effect of different excitation amplitude, stationary rings mass, axial damping, and linear stiffness on the stationary axial displacement response in the frequency domain in the presence of nonlinear stiffness. It can be seen that not only is the frequency close to the natural frequency of the system but also the displacement amplitude of the stationary rings is the largest, and at the lower frequency, the stationary rings response amplitude jumps. The reason for this is that there is a large nonlinear stiffness. It can be seen from Figure 3(a) that the system parameters (stationary ring mass, axial damping, and linear stiffness) are fixed, corresponding to the same frequency; the larger the excitation amplitude, the larger is the magnitude of the displacement response of the stationary ring. Further, with the increase in the excitation amplitude, the nonlinear characteristics of the system are enhanced. Compared with the frequency-response function curve of the smaller amplitude excitation, it shows a certain degree of right deviation. Figure 3(b) shows that the parameters (excitation amplitude, axial damping, and linear stiffness) are fixed, in the resonance region; as the mass of the stationary rings decreases, the output frequency response of the system changes nonlinearly, showing a certain degree of right deviation. Figure 3(c) shows that the parameters (excitation amplitude, stationary ring mass, and linear stiffness) are fixed and the effect of damping on the magnitude of the stationary ring displacement response. In the resonance range, as the axial damping increases, the output-response peak value $Y(jw)$ gradually decreases, that is, increasing the axial damping of the system is beneficial to attenuating the stationary rings' common amplitude value. Figure 3(d) shows that the parameters (excitation amplitude, stationary ring mass, and axial damping) are fixed; the greater the linear stiffness, the greater is the nonlinearity of the system, compared with the output frequency-response curve of the smaller axial stiffness of the system, which exhibits a degree of right deviation. In the resonance range, as the axial stiffness increases, the output response peak value $Y(jw)$ gradually increases.

4.3. Stationary Ring Response under Noise Excitation. In this section, the response output spectrum of two frequency harmonic excitation couplings is analyzed to explain further the influence of the excitation amplitude and system inherent parameters on the output displacement of the noncontact mechanical seal stationary rings. For ease of analysis, assume that the magnitudes of the two excitations are the same.

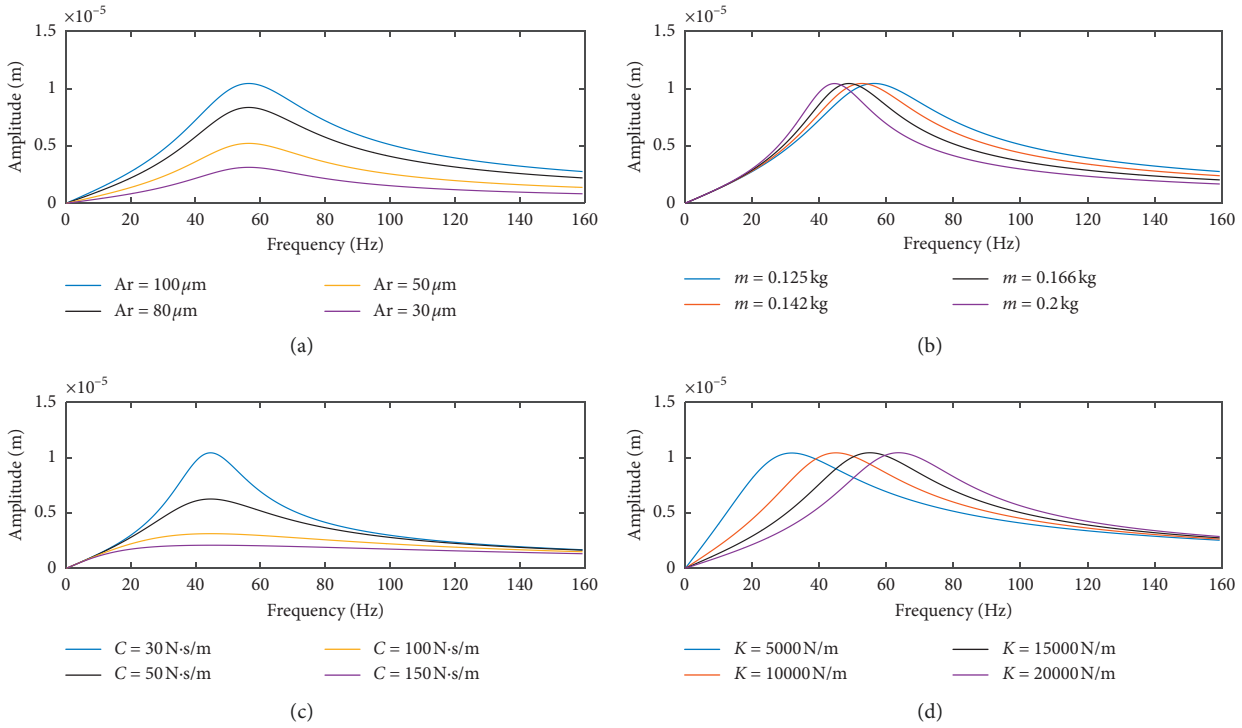

Figure 2: Analysis of influencing factors of linear operation stationary rings displacement: (a) effect of axial excitation amplitude on displacement; (b) effect of stationary ring mass on displacement; (c) effect of axial damping on displacement; (d) effect of linear stiffness on displacement.

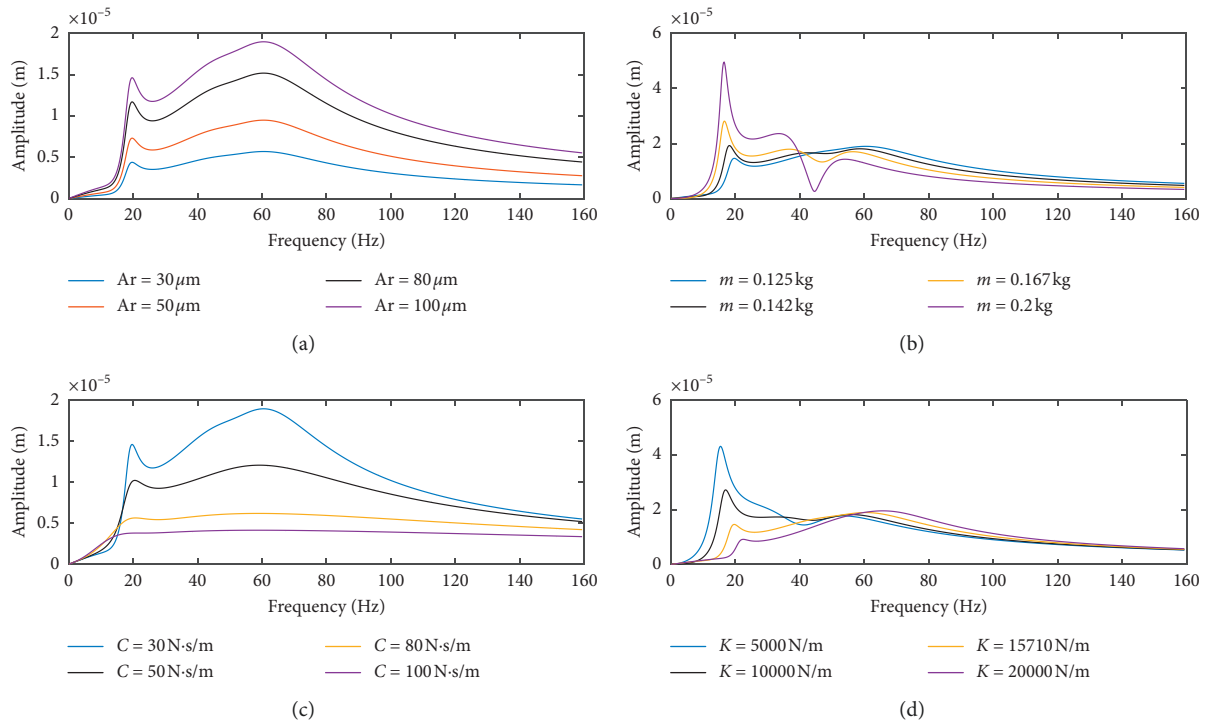

Figure 3: Analysis of influencing factors of stationary ring displacement in nonlinear operation: (a) effect of axial excitation amplitude on displacement; (b) effect of stationary ring mass on displacement; (c) effect of axial damping on displacement; (d) effect of linear stiffness on displacement.

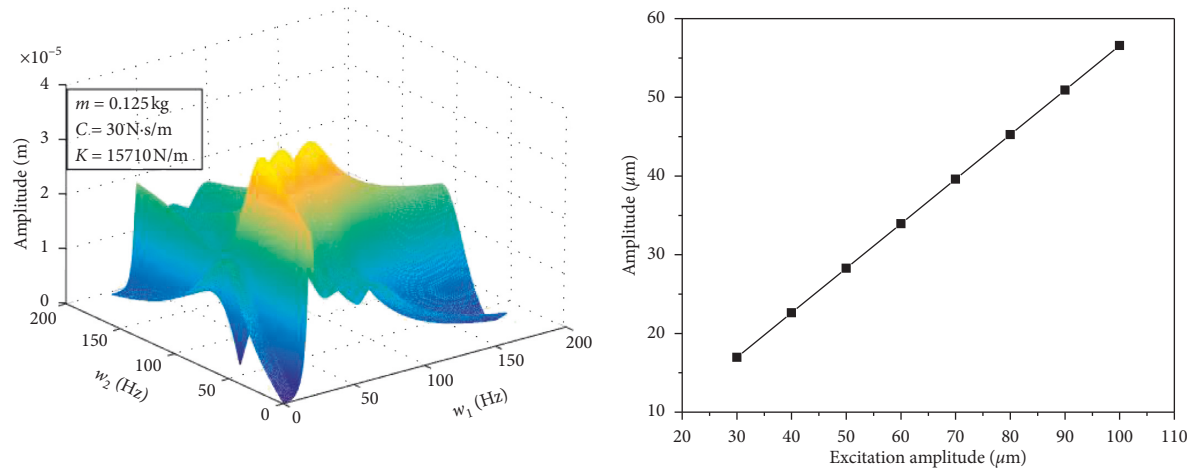

(a) (b)

Figure 4: Effect of excitation on the output spectrum. (a) Nonlinear output spectrum with Ar = 30 μm. (b) Relationship between excitation amplitude and response peak.

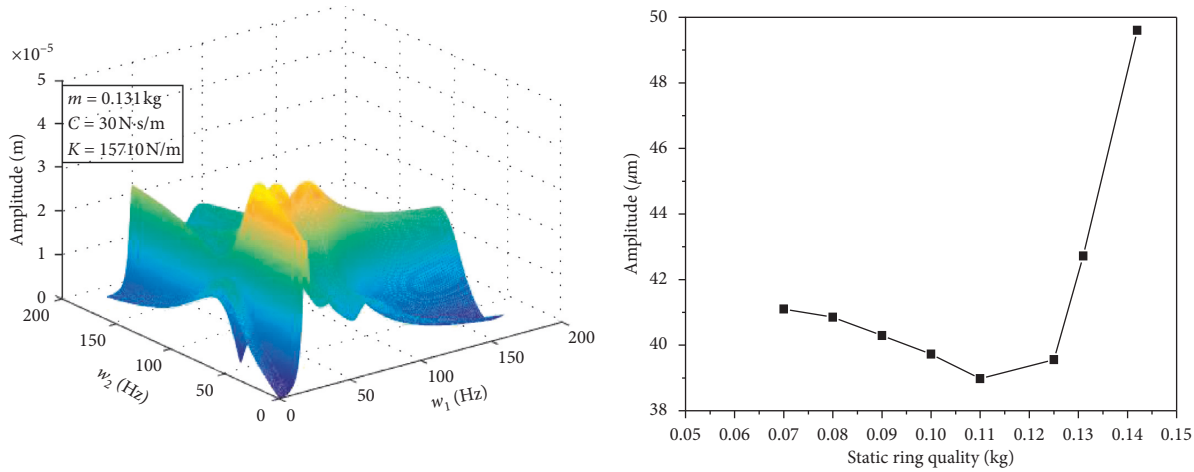

(a) (b)

Figure 5: Quality impact on the output spectrum. (a) Nonlinear output spectrum with $m = 0.131$ kg. (b) Relationship between quality and response peaks.

4.3.1. Influence of Excitation Amplitude. When the excitation amplitude is Ar = 30 μm, the response output spectrum is as shown in Figure 4(a). The relationship between the excitation amplitude and the response peak is shown in Figure 4(b). As can be seen from the figure, the excitation amplitude is linear with the response peak. This is because the Volterra frequency domain kernel (frequency response function) is the ratio of the system output to the input Fourier transform. The ratio of excitation to response is independent of the magnitude of the excitation amplitude. The Volterra frequency domain kernel contains system parameters m, C, K, and b, so it can completely contain the motion characteristics of the system.

4.3.2. Quality Impact. When the mass of the noncontact mechanical seal stationary ring is set to $m = 0.131$ kg, the response output spectrum is as shown in Figure 5(a). The relationship between mass and response peak is shown in Figure 5(b). It can be seen from the figure that when the other parameters C, K, and b of the system are constant, the response peak is slightly smaller with the increase in the stationary ring mass. When the mass increases to a certain value, the response peak increases nearly linearly. This is because when the quality of the stationary rings is smaller and the values of the parameters C, K, and b contained in the Volterra frequency domain core are large, the influence of the quality factor is small.

4.3.3. Effect of Damping. When the total axial damping of the noncontact mechanical seal is set to $C = 50$ N S/m, the response output spectrum is as shown in Figure 6(a). The relationship between the damping and the response peak is shown in Figure 6(b). It can be seen from the figure that when the damping is small, the response peak decreases

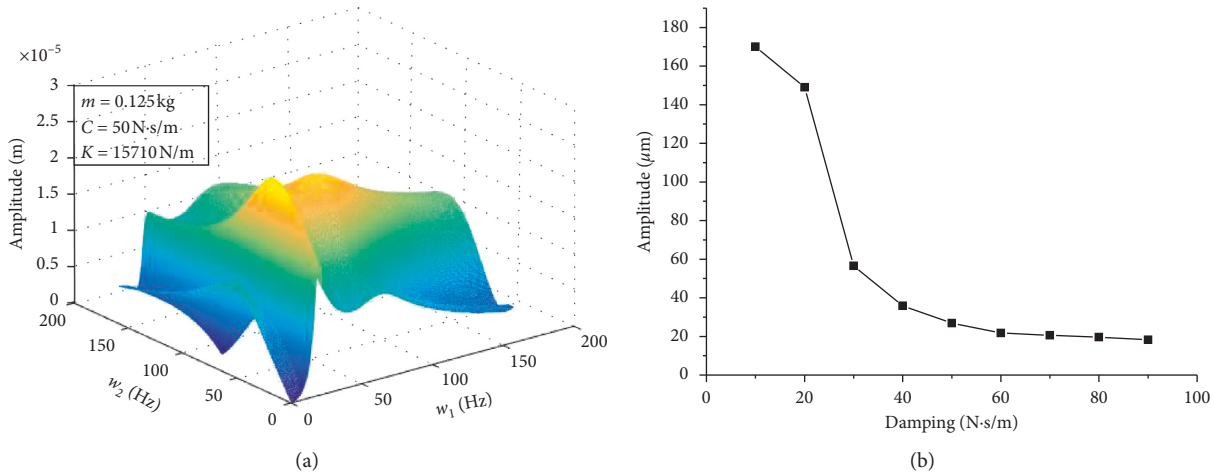

Figure 6: Effect of damping on the output spectrum. (a) Nonlinear output spectrum of $C = 50$ N·s/m. (b) Relationship between damping and response peaks.

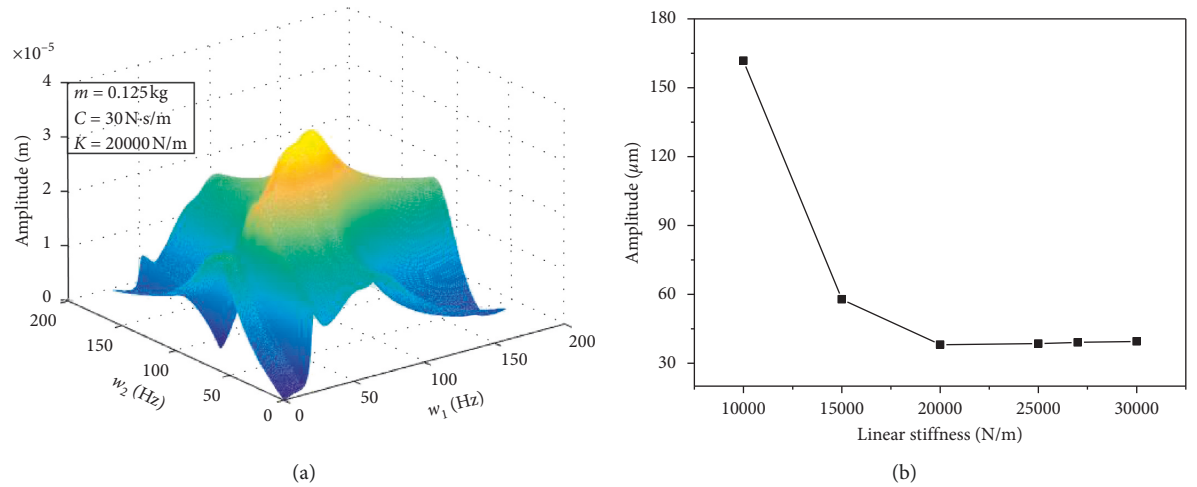

Figure 7: Effect of stiffness on the output spectrum. (a) Nonlinear output spectrum with $K = 20000$ N/m. (b) Relationship between linear stiffness and response peak.

Table 1: Symbol description.

b	Axial nonlinear stiffness (N/m^3)
C, C_1, C_{din}	Total axial damping, O-ring damping, and film damping (N·s/m)
K, K_{sp}, k_1, k_2	Axis total stiffness, spring stiffness, O-ring stiffness, and film stiffness (N/m)
m, M_R, M_{sp}	The mass of stationary rings, rotating mass, and follower (sleeve, O-ring, and spring) (kg)
R	Friction (N)
W	Frequency (Hz)
y	Stationary ring displacement (m)

sharply with the increase in damping. As the damping increases to a certain value, the magnitude of damping in response peak decreases. This is because when the damping is small, the stationary rings must slowly decrease the amplitude after a plurality of vibrations. When the damping is large, the energy is rapidly attenuated.

4.3.4. Influence of Linear Stiffness. When the total axial linear stiffness of the noncontact mechanical seal is set to 20000 N/m, the response output spectrum is as shown in Figure 7(a). The relationship between linear stiffness and response peak is shown in Figure 7(b). It can be seen from the figure that the maximum peak of the output response decreases sharply with increasing linear stiffness. When the linear stiffness reaches a certain value, the maximum peak value of the output response increases slightly with increasing stiffness. The reason is that after the linear stiffness reaches a certain value, the influence on the stationary ring amplitude is mainly nonlinear stiffness.

5. Conclusion

(1) The axial excitation amplitude, linear stiffness of the system, damping, mass of the stationary rings, and nonlinear stiffness have a greater influence on the

amplitude of stationary rings. Therefore, in order to ensure the optimum performance of the noncontact mechanical seal, it is necessary to take effective measures to control the axial excitation amplitude strictly.

(2) As the nonlinear stiffness acts significantly in the low-frequency region, it is avoided to prevent the noncontact mechanical sealing system from working in the low-frequency region.

(3) In the low-frequency region, the amplitude of the stationary rings can be effectively controlled by using a stationary ring with smaller mass, larger damping, and larger linear stiffness so as to reduce the leakage amount.

(4) In the high-frequency region, the amplitude of the stationary rings can be effectively controlled by using a stationary ring with larger mass, larger damping, and smaller linear stiffness so as to reduce the leakage amount (Table 1).

Data Availability

All data included in this study are available upon request by contacting the corresponding author.

Conflicts of Interest

The authors declare that they have no conflicts of interest.

Acknowledgments

This article was supported by the National key Research and Development Plan (2018YFB2000800) and National Key R&D Program of Jiangsu Province (BE2017026).

References

[1] L. P. Ludwig and R. C. Bill, "Gas path sealing in turbine engines," *A S L E Transactions*, vol. 23, no. 1, pp. 1–22, 1980.

[2] Y. C. Liu, Z. Lu, and X. M. Shen, "The development of gas film face seal in advanced aero-engine," *Journal of Mechanical Science and Technology*, pp. 639–645, 1998.

[3] X. K. Meng, X. D. Peng, and L. Q. Wang, "Axisymmetric dynamic model and seal behavior analysisofmechanical seals during startup and shutdown operation," *CIESC Journal*, vol. 62, no. 6, pp. 1620–1625, 2011.

[4] X. X. Ding, H. Z. Zhang, H. Su et al., "Axial vibration response of a two-degree-of-freedom system with dry-gas seal," *Journal of Vibration Measurement & Diagnosis*, vol. 33, no. S2, pp. 77–80, 2013.

[5] S. V. Falaleev and A. S. Vinogradov, "Analysis of dynamic characteristics for face gas dynamic seal," *Procedia Engineering*, vol. 106, pp. 210–217, 2015.

[6] P. Varney and I. Green, "Steady-state response of a flexibly mounted stator mechanical face seal subject to dynamic forcing of a flexible rotor," *Journal of Tribology*, vol. 139, no. 6, Article ID 062201, 2017.

[7] S. T. Hu, W. F. Huang, X. F. Liu et al., "Transient response analysis of spiral groove gas face seals under pressure-drop fluctuation," *Journal of Fluid Mechanics*, vol. 45, no. 2, pp. 22–27, 2017.

[8] R. R. Badykov and S. V. Falaleev, "Advanced dynamic model development of dry gas seal," *Procedia Engineering*, vol. 176, pp. 344–354, 2017.

[9] F. He and Y. Z. Zhu, "Motion analysis and stability of end seals," *Journal of Fluid Mechanics*, vol. 1, no. 1, pp. 21–26, 1989.

[10] I. Green and R. M. Barnsby, "A simultaneous numerical solution for the lubrication and dynamic stability of non-contacting gas face seals," *Journal of Tribology*, vol. 123, no. 2, pp. 388–394, 2001.

[11] I. Green, "Gyroscopic and support effects on the steady-state response of a noncontacting flexibly mounted rotor mechanical face seal," *Journal of Tribology*, vol. 111, no. 2, pp. 200–206, 1989.

[12] S. Blasiak, "Numerical analysis of the non-contacting gas face seals," *IOP Conference Series: Materials Science and Engineering*, vol. 233, no. 1, Article ID 012032, 2017.